

Design Guidelines for Luminescent Solar Concentrator Greenhouses in the United States

Kristine Q. Loh, Kale Harbick, Nathan J. Eylands, Uwe R. Kortshagen, and Vivian E. Ferry**

Agrivoltaic greenhouses combine controlled environment agriculture and photovoltaics in one plot of land to simultaneously address the global challenges of renewable energy and sustainable food production.

Luminescent solar concentrators (LSCs) benefit these systems by providing additional design flexibility, tuning light transmission for plant growth while generating electricity. Herein, design guidelines for LSCs in agrivoltaic greenhouses are determined given the two competing priorities of light utilization, crop yield and energy generation. Using a comprehensive model, the impact of LSC design choices on the greenhouse environment, energy generation, crop yield, and economic value in 48 locations across the United States is evaluated. It is shown that the solar cell coverage ratio and the greenhouse's heating demands determine the energy offset provided by the LSC. For improving crop yield, luminophore selection should maximize transmitted red light. The sensitivity of the economic value to crop yield, thus dictating luminophore selection for optimizing plant growth, is demonstrated. LSC greenhouses are as profitable as conventional greenhouses generally for states below 40 °N. Future improvements to LSC manufacturing may allow previously unprofitable LSC greenhouses to become economically viable in northern states. This work showcases the broad design space and strong potential for LSCs in agrivoltaics.

population of 10 billion people by 2050, augmentation of the agricultural industry is critical for sustainable economic growth.^[1] Yet, due to climate change stressors, food production systems are strained due to decreasing arable land and harmful changes to outdoor growing conditions.^[2] Greenhouse cultivation provides one solution to this problem, as the enclosed environment protects crops from adverse environmental conditions.^[3] In addition, the controlled environment allows for year-round crop production, in contrast to seasonal traditional farming methods. However, greenhouses consume significant amounts of energy for heating, especially in colder climates, leading to high operational costs and additional greenhouse gas emissions from traditional heating methods.^[4,5]

Agrivoltaic systems promote dual land use by strategically combining photovoltaics (PV) and agriculture.^[6–8] In these systems, agriculture and PV installations coexist and are even symbiotic; the shading under PV panels aids in

crop water retention while water vapor released through transpiration assists in panel cooling.^[9] With the rapidly declining price of crystalline silicon PV modules,^[10] much of the agrivoltaics community has focused on integrating Si PV modules in different configurations and locales.^[11,12] Typical agrivoltaic

1. Introduction

With the growing global population, there is a rising need for both renewable energy generation and increased food production to sustain larger communities. To meet a projected global

K. Q. Loh, V. E. Ferry
Department of Chemical Engineering and Materials Science
University of Minnesota
Minneapolis, MN 55455, USA
E-mail: veferry@umn.edu

K. Harbick
Application Technology Research Unit
USDA ARS
Toledo, OH 43606, USA
N. J. Eylands
Department of Horticultural Science
University of Minnesota
St. Paul, MN 55108, USA
U. R. Kortshagen
Department of Mechanical Engineering
University of Minnesota
Minneapolis, MN 55455, USA
E-mail: kortshagen@umn.edu

 The ORCID identification number(s) for the author(s) of this article can be found under <https://doi.org/10.1002/adsu.202400749>

© 2024 The Author(s). Advanced Sustainable Systems published by Wiley-VCH GmbH. This is an open access article under the terms of the Creative Commons Attribution-NonCommercial-NoDerivs License, which permits use and distribution in any medium, provided the original work is properly cited, the use is non-commercial and no modifications or adaptations are made.

DOI: [10.1002/adsu.202400749](https://doi.org/10.1002/adsu.202400749)

installations involve PV modules installed at a specific height and angle depending on the crop height and light requirements. One additional application space is in greenhouses, where PV glazing offsets high energy demands from greenhouse operations.^[13] The installation of the PV cells on the greenhouse roof and/or walls depends on the type of crop grown in the greenhouse. For crops that need higher light conditions, transparent or semi-transparent PV cells can be designed to transmit as much light as possible but suffer from low power conversion efficiencies (PCEs) due to reduced PV cell area.^[14,15] In contrast, fully opaque PVs generate more electricity at the expense of light transmission, thereby reducing crop photosynthesis.^[16] Nevertheless, the full picture of the influence of PV cells and modules on crop growth in different environments is the subject of current research.

Luminescent solar concentrators (LSCs) have received growing interest in the agrivoltaics community, as the spectral shaping of transmitted light can benefit crop yield in addition to the concentration of light onto small-area PV cells.^[17–23] LSCs consist of a waveguide doped or coated with luminophores (fluorescent dyes, quantum dots (QDs), etc.) that absorb and re-emit a fraction of incident sunlight. The photoluminescence is guided to surrounding small-area solar cells via total internal reflection, resulting in both concentration and spectral shifting of high-energy sunlight to longer wavelengths that are more efficiently converted to electricity by the solar cell.^[24] LSCs operate well in both diffuse and direct lighting, eliminating the need for a solar tracking system.^[25] Furthermore, LSCs use commercially available Si PV cells. While an LSC will practically have a lower PCE than a crystalline Si PV cell of the same area, the design flexibility granted by modifying the waveguide or the luminophore to control color and transparency makes LSCs an excellent option for agrivoltaic systems. Integrating LSCs into greenhouse roofs presents a promising opportunity to provide clean energy while benefitting crop yield; however, the LSC design considerations that balance transmission and electricity generation as well as the impacts on the greenhouse environment need to be better understood.

This work develops design guidelines for implementing LSCs in agrivoltaics, using a model that evaluates the trade-off between light used for energy generation and for crop growth in LSC greenhouses. To understand the competing priorities for LSC greenhouses, we first model the impact of transmitted light spectra determined by the luminophore choice and concentration on the growth of Bibb lettuce. Then, we model LSC greenhouse energy balances^[23] to compare the amount of energy supplied and demanded by LSC greenhouses depending on the LSC film dimensions related to the PV coverage ratio. As the primary figure of merit, the net present value (NPV) for each simulated greenhouse is calculated to assess the economic impacts of the light trade-off depending on the crop selling price and the cost of metering. Finally, we identify the key technological improvements, namely longer LSC lifetimes and lower costs, that could bring the realization of LSC greenhouses closer to fruition, even in cold climates. Our analysis provides insight into the design guidelines for LSC greenhouses and shows that these designs could allow for enhanced profit in addition to the sustainability benefits of solar energy technology.

2. Experimental Section

This model incorporates solar resources with models for heat and energy, power generation, lettuce (cv. Rex) crop yield, and economic models. Two periodic LSC roof structures are considered: a small-area 8 cm x 8 cm LSC film and a larger-area 16 cm x 16 cm film, each surrounded by 2 cm-wide PV cells (36% and 21% PV coverage, respectively). The LSC greenhouses also had LSC films covering the walls. These were benchmarked against a conventional glass greenhouse. For all greenhouse structures, 20% of incident light was blocked by framing structures on the walls.^[26]

An overview of the model is represented in **Figure 1**. First, transmission of incident sunlight through all parts of the greenhouse was modeled. A fraction of the incident sunlight was used to generate electricity in LSC greenhouses, and the power generated was modeled accordingly. Then, a greenhouse environmental model developed in previous work to determine heating and cooling demands for the greenhouse, as well as hourly indoor temperatures, was used.^[23] Heating and cooling demands depended on the sunlight entering the greenhouse and the ambient temperature. Next, hourly crop growth considering light spectrum, light intensity, and the temperature of the crop layer was modeled. Lastly, an economic model to weigh all the model outputs was used.

2.1. Optical Modeling and LSC Roof Structure

Using data retrieved from the NASA POWER Database, the hourly sunlight transmitted and absorbed through the roof and walls of the greenhouse based on a solar resources and optical model used in the previous work was determined.^[23,27] Briefly, the roof structure consists of a grid of front-facing PV cells with luminescent films in the blank spaces. The film and PV cells are attached underside a glass panel with refractive index matching adhesives. This design allows the PV cells to absorb both waveguided PL from the luminescent film and direct solar radiation. Data were retrieved to model greenhouses in 48 locations in the contiguous United States. Additional geographic information is detailed in Table S6 (Supporting Information). Using the retrieved daily averaged data, hourly beam, diffuse, and ground-reflected radiation were modeled.^[23,28]

Three nontoxic luminophores previously evaluated for LSC roofs were also studied: copper indium sulfide/zinc sulfide quantum dots (CIS/ZnS),^[29,30] silicon quantum dots (Si),^[17,23] and Lumogen Red 305 molecular dye (LR305).^[18,19,30,31] Absorbance and photoluminescence (PL) spectra, as well as the PL quantum yield (PLQY), were retrieved from the literature.^[32–34] In this work, CIS/ZnS QDs had the highest PLQY of 85%, while LR305 and Si QDs had PLQY values of 80% and 60%, respectively. While previous reports show that these values could be higher, reaching almost 100% for LR305,^[35] the PLQY values used here correspond to the retrieved absorption and PL data. Higher PLQY values mean that fewer photons are lost to nonradiative recombination; the emitted photons may be collected by the solar cell but may also be lost to other pathways such as reabsorption and escape cone emission.^[36] An example of transmitted spectra through the LSC films as compared to the AM1.5G solar spectrum is shown in

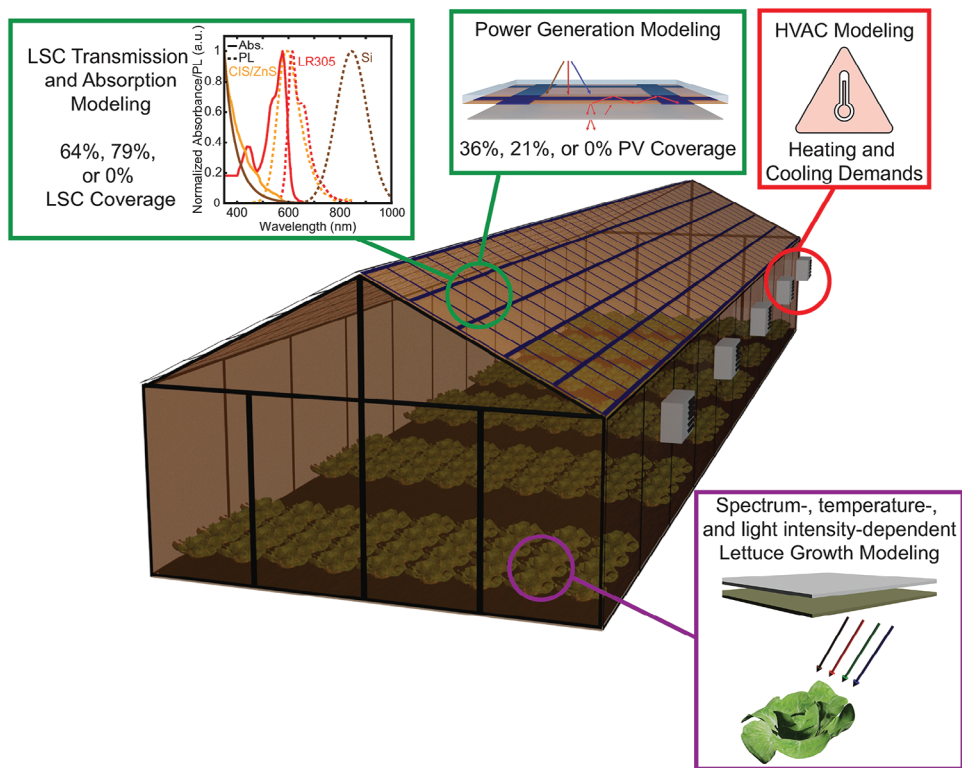


Figure 1. Overview of the model presented in this work.

Figure S1 (Supporting Information). The concentration of these luminophores to balance light transmission for crop growth and light reflected via total internal reflection in the LSC for energy generation was varied. The loading for all luminophores was varied such that the optical density at 450 nm ranged from 0.1 to 2.0 at step sizes of 0.1 in the four representative locations discussed in detail below and 0.25 to 2.0 at step sizes of 0.25 in the 48 continental U.S. locations.

2.2. Greenhouse Structure and Environmental Modeling

All greenhouses simulated were designed with the same construction as an A-frame style greenhouse that was 29.3 m long and 7.3 m wide (96 ft x 12 ft).^[37] The gutter height was 3.1 m, and the roof was sloped at 27°.^[38] All simulated greenhouses were also oriented north-south, and the north-facing wall was assumed to be an adiabatic surface to represent a headhouse.^[39,40] All other walls were assumed to be made of 3 mm thick glass. The indoor temperature setpoints were 21–28 °C during the day and 17–18 °C at night. The relative humidity inside the greenhouse was also controlled to be below 80%.^[23]

Inside the greenhouse, all surfaces were covered with a diffuser film to reflect growing best practices, where diffuser films converted incident light into diffuse light to penetrate multiple layers of the plant for improved growth.^[41] This nonspectrally dependent diffuser film transmitted 90% of incident light^[42] and reduced convective heat transfer by adding an air space between the

glass and the film.^[43] Furthermore, shades were deployed during the day at gutter height to control the extended daily light integral (eDLI). The eDLI describes the number of photons in the extended photosynthetically active radiation (ePAR) range of 400–750 nm incident on the crop over 24 h. Following an hourly shading algorithm developed by Albright et al.,^[26] shades were used during the day to meet a target eDLI of 19 mol m⁻² d⁻¹. This target was chosen to provide sufficient light for crop growth without risking tip burn at high eDLI values. Shades were also deployed at night to regulate the greenhouse temperature based on the typical growing season for lettuce in that location.^[44]

The transmittance of the shade cloth for each simulated greenhouse was intentionally chosen to meet an average annual eDLI. For the conventional greenhouses, the shade cloth transmittance solely depended on the location's hourly insolation. However, for the LSC greenhouses, the luminophore optical density must be considered as well. As the optical density increased, the shade cloth transmittance was also increased to compensate for the increased light absorption by the LSC films. The two PV coverage ratios studied in this work impacted the choice in shade cloth transmittance as well, and the greenhouses with the higher coverage ratio required higher shade cloth transmittances to compensate for the light blocked by the PV cells. These trends are shown for four representative locations in Figure S3 (Supporting Information). Figure S4 (Supporting Information) through Figure S7 (Supporting Information) shows the resulting daily eDLI values for LSC greenhouses in each of the representative locations.

2.3. Crop Growth Modeling

As the use of LSCs in the greenhouse increased light competition, a low-light tolerant crop as the focus of this analysis was used. As the primary greenhouse lettuce type, Bibb or Butterhead lettuce has been used as the crop of interest in multiple controlled environment agriculture feasibility studies.^[45–48] The most common growth model for estimating lettuce yield is the Van Henten model.^[49] However, this model does not consider the impact of the light spectrum on growth, despite recent literature that emphasized its importance.^[50,51] Furthermore, a primary advantage of LSCs in the agriculture space is spectrum shifting and control.^[29,30,52] The model developed by Abedi et al. that considers incident light spectrum on lettuce growth to model Bibb lettuce (cv. Rex) that was harvested every 35 days was used.^[53] To reflect growing best practices, a planting density of 24 plants m⁻² was assumed. The dry biomass was also assumed to account for 10% of the fresh weight (FW) at harvest.

2.4. Economic Framework

The NPV for each simulated greenhouse was calculated as the primary figure of merit in this work. The NPV considered capital costs, variable costs, income from crop revenue, and credits from net metering.^[54] For calculating crop revenue, the lettuce price was varied from \$0.30 to \$1.80 per head to encompass a variety of markets and selling prices, from wholesale to farmer's markets. Assuming one head of Bibb lettuce is roughly 150 g, the lettuce prices varied from \$2 to \$12 kg⁻¹. Furthermore, it was assumed that any heads smaller than 150 g were sold as chopped baby lettuce leaves at the same range of prices.^[55]

An interest rate of 10% and a lifetime of 30 years for all NPV calculations were assumed.^[56] For the costs incurred in installing the LSC roofs, a standard price for the luminophore films depending on the surface area required was assumed. Furthermore, unless specified otherwise, the films were repurchased every 5 years to reflect the lifetime of luminophore films on the market.^[57] For the LSC greenhouses, the cost of the PV cells was calculated by multiplying a levelized cost of electricity by the amount of power generated by the cells.^[58]

The relative NPV compares the NPV of the LSC greenhouse to that of the conventional greenhouse. Positive relative NPVs indicated that the LSC-PV greenhouse was more profitable than the conventional greenhouse. Negative relative NPVs indicated that the LSC-PV greenhouse was less profitable than the conventional greenhouse, but may still produce an actual profit. All relative values were in reference to the relevant results for conventional glass greenhouses.

More information for all calculations can be found in Supporting Information and Figure S2 (Supporting Information) portrays all relevant model input and output variables. All simulations and calculations were conducted in MATLAB.

3. Results and Discussion

3.1. Energy Generation and Demand in LSC Greenhouses

First, we studied the impact of luminophore loading on energy generation and the potential for net zero energy (NZE)

greenhouses, where the total energy demand was met by the power produced by the PV cells. Figure 2 shows the annual energy generated for simulated LSC greenhouses in four representative locations (Phoenix, Arizona (AZ), Fort Lauderdale, Florida (FL), Minneapolis, Minnesota (MN), and Lancaster, Pennsylvania (PA)) to understand the impact of varying sunlight and ambient temperature on greenhouse operation. These locations represented the four main Koppen–Geiger (KG) climate classifications at a broad range of latitudes in the continental United States (arid, equatorial, warm temperature, snow).^[59] Greenhouses in AZ received the most sunlight while greenhouses in FL, MN, and PA received comparable amounts of sunlight. Greenhouses in AZ, MN, and PA experienced sub-freezing ambient temperatures, but the climate in FL was more temperate. These differences in climate impacted the greenhouse energy demands, as shown in Figures S8 and S9 (Supporting Information), with LSC greenhouses in locations with sub-freezing temperatures requiring most of their energy from heating. Table S7 (Supporting Information) lists the heating and cooling demands for conventional greenhouses in each simulated location.

As the optical density of the luminophores increased, more incident sunlight was absorbed, and more photons are directed toward the adjacent PV cells, resulting in increasing energy generation (as well as more photons to other loss pathways). LR305, with its larger spectral overlap between absorption and PL, exhibited limited energy generation at higher optical densities due to self-absorption losses. Si, despite its lower PLQY, generated comparable amounts of energy at higher optical densities because of the minimal overlap between its absorption and PL spectra. CIS/ZnS, with the highest PLQY of the three and limited spectral overlap, consistently produced the most energy. Therefore, luminophores that have high PLQY values and limited self-absorption losses will improve energy generation, as has been discussed in previous analyses of LSCs.^[60]

From an LSC structure design perspective, the PV coverage ratio and the annual heating demands of the greenhouse determined whether the greenhouse was NZE. All 8 cm x 8 cm LSC greenhouses in both AZ and FL were NZE due to the higher PV coverage ratio of 36%, as shown in Figure 2a,b. Yet, only the 16 cm x 16 cm LSC greenhouse in FL in Figure 2b was NZE as the greenhouses in AZ had higher heating demands to combat subfreezing temperatures in the winter. While all LSC greenhouses in MN and PA could generate energy, shown in Figure 2c,d, none of them were NZE due to the high heating demands in the winter. The 8 cm x 8 cm LSC greenhouses supply ≈10% and 25% of the total energy demand in MN and PA, respectively. With the lower PV coverage ratio, the 16 cm x 16 cm LSC greenhouses supply even less. Due to the required increase in shade cloth transmittance to meet the target eDLI, the increased heating demand upon application of LSC films to the greenhouse surpasses the amount of energy generated for greenhouses in both MN and PA, shown in Figures S8c,d and S9c,d (Supporting Information). From an energy perspective, LSC design that results in a higher PV coverage ratio could lead to NZE greenhouses, but the implementation of LSCs for cold-climate greenhouses leads to increased energy demands that cannot be offset.

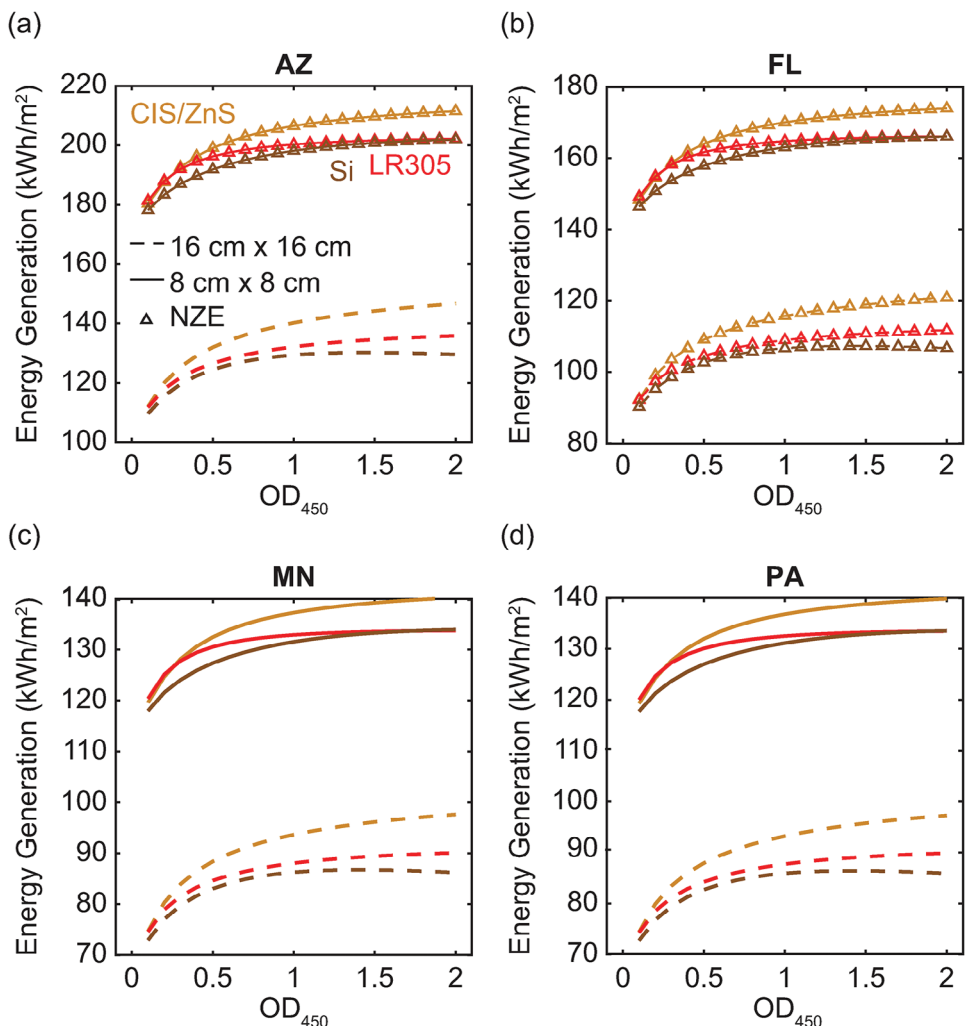


Figure 2. Annual energy generation for CIS/ZnS, LR305, and Si LSC greenhouses in a) AZ, b) FL, c) MN, and d) PA as a function of luminophore optical density at 450 nm. Solid lines represent energy generated by 8 cm x 8 cm LSC greenhouses while dashed lines show energy generated by 16 cm x 16 cm LSC greenhouses. Additional triangles indicate LSC greenhouses that generated more than the total energy demand, or were NZE.

3.2. Lettuce Growth in LSC Greenhouses

Upon studying the LSC greenhouses from an energy-focused standpoint, we then turn to understanding the benefits and challenges of utilizing LSCs from a crop growth perspective. We determined the influence of the luminophore absorption, PL spectra, and optical density in the LSC films on lettuce growth. As an example for a set of input and output data that are used for the analysis of greenhouses at one location, **Figure 3** depicts the shade cloth transmittances chosen for varying optical densities of 8 cm x 8 cm Si LSC greenhouses and the conventional greenhouse in AZ to demonstrate the impact of these two variables on average annual eDLI and annual fresh weight. Through intentional selection of the shade cloth transmittance, the average annual eDLI was maintained to meet the target eDLI, unless the optical density was too high (above 1.8 in this case). At these highest optical densities, 100% transmittance shade cloths were required as the LSC films absorbed too much light to meet the target eDLI. The optical density at which 100% transmittance shade

cloths were required depended on the amount of incident sunlight, or the location of the greenhouse. In contrast to the higher irradiance in AZ, most or all of the LSC greenhouses in locations with less sunlight required highly transmissive shade cloths. Despite the maintenance of the average annual eDLI at optical densities below 1.8, Figure 3b illustrates the annual fresh weight changes with optical density because of the changing transmitted spectrum. Because Si primarily absorbs UV/blue light and emits red/near infrared (NIR) light, increasing the optical density of Si increases the ratio of red light and decreases the ratio of blue light in the transmitted spectrum. As a result, the fresh weight increases as well in agreement with previous experiment studies.^[61]

To highlight the differences between crop growth in LSC greenhouses in warm and cold climates, **Figure 4** depicts the influence of LSC size, luminophore choice, and optical density on annual crop yields in AZ and MN. Figure S10 (Supporting Information) shows the annual fresh weights for greenhouses in FL and PA as well. In AZ, despite comparable average annual

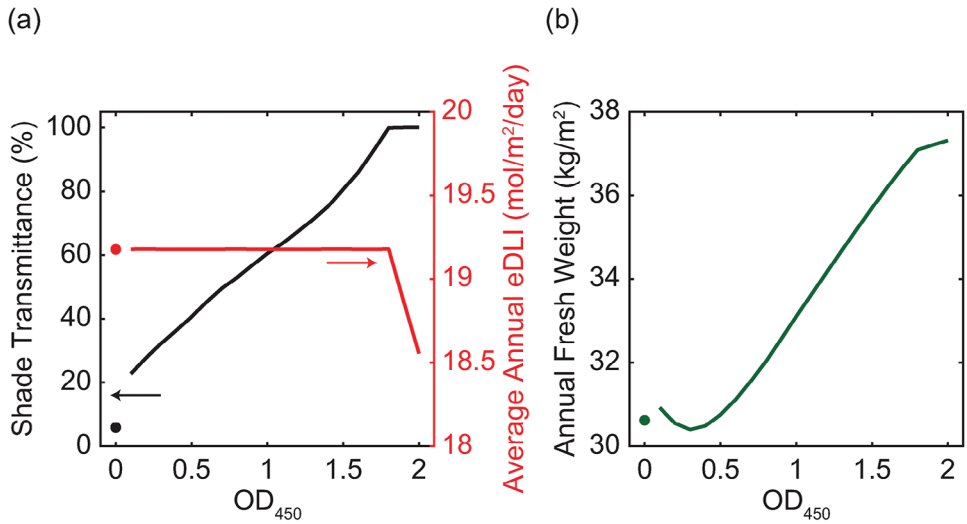


Figure 3. a) Shade cloth transmittance chosen for varying Si optical density in 8 cm x 8 cm LSC greenhouses in AZ alongside the resulting average annual eDLI and b) annual fresh weight. Inputs and outputs for the conventional greenhouse are plotted as circular markers at an optical density of 0 as a reference.

eDLI values, the resulting annual fresh weight differed across the greenhouses with LSC films of different optical densities, as shown in Figures 3b and 4a. In warm climates, we can then attribute these differences to the influence of spectrum shifting on crop growth. Figure S11 (Supporting Information) shows that with increasing optical density, the red fraction increases as well for all LSCs in all locations. LR305 LSC greenhouses have the highest red fraction in the transmitted light due to the combination of the peak of the PL spectrum being in the red range of the visible spectrum and the peak of the absorbance spectrum being in the green range. As a result, LR305 LSC greenhouses produce the most lettuce at the optical density that balances higher red fractions with sufficient light for crop growth.

These findings agree with those of Camporese and Abou Najm, who also modeled basil and strawberry under agrivoltaic panels and found that these crops better utilized red light.^[62] The yields for the QD LSC greenhouses are comparable to each other, suggesting the absorption spectra of the luminophore drives crop yield.

Although the red fractions were nearly the same between the two LSC sizes studied, the larger-area LR305 LSC greenhouses produced more lettuce at optical densities above 1 for greenhouses in warm climates. These differences can be attributed to differences in the crop temperature, as shown in Figure S12a,b (Supporting Information). For greenhouses with a reduced PV coverage, lower shade cloth transmittances were required to meet

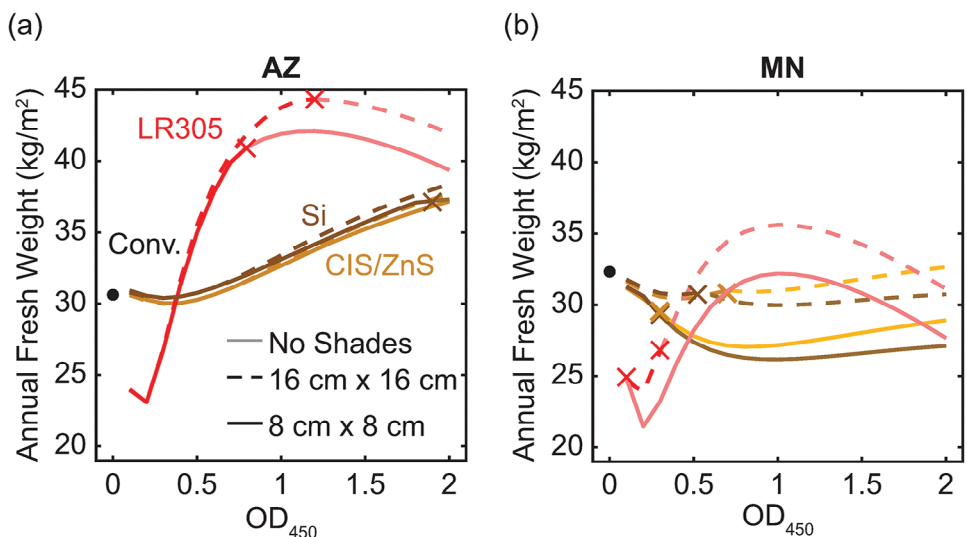


Figure 4. Annual fresh weight as a function of luminophore optical density at 450 nm for both 8 cm x 8 cm (solid lines) and 16 cm x 16 cm (dashed lines) LSC greenhouses in (a) AZ and (b) MN. Annual fresh weights for the conventional greenhouses in each location are plotted as black circles at OD₄₅₀ of 0 for reference. LSC greenhouses that required shade cloths with 100% transmittance are plotted in a lighter shade.

Table 1. Conventional greenhouse NPV in the four representative locations given \$2, \$7, and \$12 kg⁻¹ lettuce prices.

Location	Lettuce Price	NPV [\$k]
AZ	\$2 kg ⁻¹	14.6
	\$7 kg ⁻¹	382
	\$12 kg ⁻¹	847
FL	\$2 kg ⁻¹	-7.90
	\$7 kg ⁻¹	316
	\$12 kg ⁻¹	725
MN	\$2 kg ⁻¹	-16.2
	\$7 kg ⁻¹	371
	\$12 kg ⁻¹	863
PA	\$2 kg ⁻¹	2.69
	\$7 kg ⁻¹	376
	\$12 kg ⁻¹	849

the target eDLI; with the decrease in shade cloth transmittance, heat retention was improved.

In cold climates with less sunlight, like in MN, the reduction in eDLI in the winter months dominates the influence of the LSCs on crop growth, as shown in Figure S6 (Supporting Information). Although the eDLI increases in the summer, the loss of crop yield in the winter months reduces the overall annual fresh weight. Despite the increase in red fraction, only the larger-area LR305 LSC greenhouses could produce more lettuce than the conventional greenhouse, as depicted in Figure 4b. In this case, the improvements to red fraction without significant hindrance to the eDLI led to improvements in plant growth. The crop yields in the QD LSC greenhouses showed similar trends, with the red fraction not being high enough to compensate for the drop in eDLI. Regarding LSC design guidelines for crop growth, luminophores that increase the red fraction at a concentration that does not significantly reduce light transmission will improve crop yield.

3.3. Competing Economic Priorities for LSC Greenhouses

To assess the tradeoff between light used for energy generation and light used for crop growth, we evaluate the economic potential of each simulated greenhouse, thus combining both greenhouse outputs into one figure of merit. By varying both the cost of metering and lettuce price, we can place different weights on the two competing priorities of energy generation and crop yield, respectively. The economic model employed aligns with the work of Ravishankar et al., who found that crop yield was the primary economic driver for organic solar cell greenhouses.^[39] Example NPVs at low, intermediate, and high lettuce prices for conventional greenhouses in the four representative locations are listed in Table 1. Varying the lettuce price significantly impacted the NPV of the conventional greenhouse, as the range in NPVs spanned hundreds of thousands of dollars in all locations. Some conventional greenhouses with limited crop yield, such as those in FL and MN, were also only profitable above wholesale lettuce prices due to the costs incurred for constructing the greenhouse and/or the costs incurred to supply sufficient heat for temperature maintenance.

LSC greenhouses in locations with sufficient irradiation have an additional benefit of net metering compared to the conventional greenhouse due to the production of electricity that can be sold back to an electrical grid. Figure 5 illustrates relative NPVs as a function of both cost of metering and lettuce price for LSC greenhouses in both FL (all LSC greenhouses are NZE) and PA (no LSC greenhouses are NZE) selected under different economic priorities. The selection was based on the optical density that resulted in either the most lettuce or energy production for each luminophore. For example, in prioritizing lettuce production, the optimized optical density for LR305 was ≈ 1 while the optimized optical density for the QDs was 2. In FL, the relative NPV increased as both cost of metering and lettuce price increased, as there was excess electricity that could be sold through net metering. In PA, the relative NPV only changed as a function of lettuce price, similar to that of the conventional greenhouse, as there was no excess electricity that could be sold.

Figure 5a,d shows the relative NPV of the 16 cm x 16 cm LSC greenhouse that produced the most lettuce in that state. Whether the relative NPV was positive or negative depended on the opportunity for enhanced crop yield in the LSC greenhouse. In FL, all LSC greenhouses were more profitable as all luminophore choices could enhance growth. Yet, in PA, only LR305 LSC greenhouses led to increased yield; only LR305 LSC greenhouses could result in positive relative NPVs. To factor in an enhancement in energy generation with an increase in the PV coverage ratio, Figure 5b,e shows the relative NPVs of the 8 cm x 8 cm LSC greenhouses that produced the most lettuce. However, the relative NPV still primarily depended on the crop yield. In FL, the relative NPV was always positive but lower than that for the 16 cm x 16 cm LSC greenhouses due to a reduction in crop yield. In PA, none of the 8 cm x 8 cm LSC greenhouses produced more lettuce than the conventional greenhouse, so the relative NPV was always negative. The additional profit from net metering was not as significant as the potential benefit from additional crop sales.

To instead prioritize energy generation, Figure 5c,f shows the relative NPVs of the 8 cm x 8 cm LSC greenhouses that produced the most energy. As the CIS/ZnS LSC greenhouses produced the most energy, the relative NPVs for these greenhouses were the highest. Si LSC greenhouses were not as profitable, despite the comparable electricity production to the LR305 LSC greenhouses, because of the lower crop yield. Because the lettuce yield was not prioritized, the range in potential relative NPVs was the lowest among the three scenarios studied.

3.4. The Potential for LSC Greenhouses Across the United States

Upon establishing LSC design rules for both energy generation and plant growth, we then simulated 8 cm x 8 cm LSC greenhouses in 48 locations across the continental United States to understand the potential for LSC greenhouses nationwide. Figure 6 illustrates the optimum greenhouse from an economic perspective in each of these 48 locations. Figure 6a demonstrates that LSC greenhouses, particularly LR305 greenhouses with the ability to produce more crops, are the most profitable option in locations generally below 40 °N in the United States. No squares or triangles are shown in Figure 6 due to the enhanced crop yield provided by the LR305 LSC roofs. While CIS/ZnS and Si

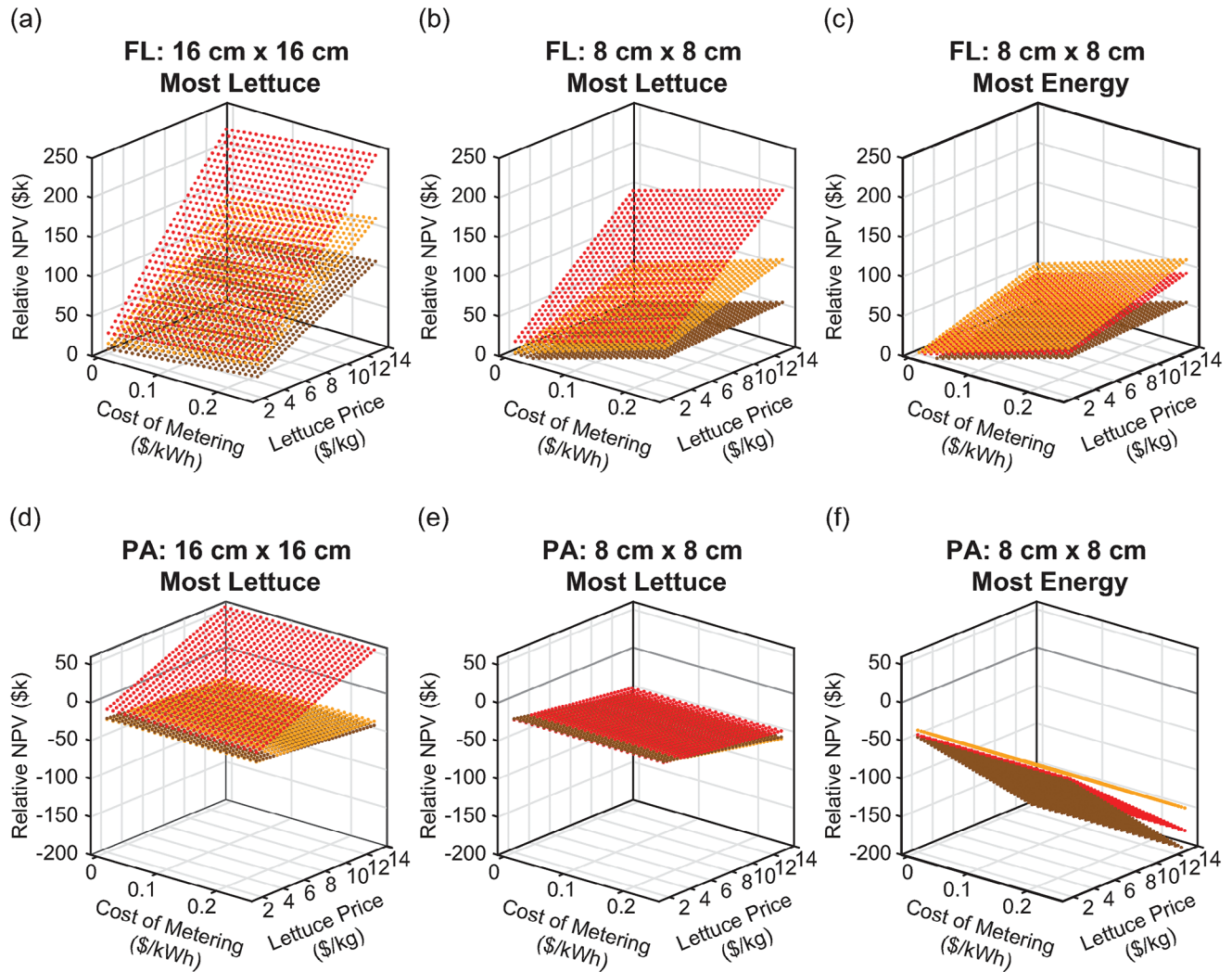


Figure 5. Relative NPV as a function of both cost of metering and lettuce price for greenhouses in FL a–c) and PA d–f). (a) and (d) show the relative NPV for 16 cm x 16 cm LSC greenhouses at the optical density that resulted in the most lettuce production. (b) and (e) show the relative NPV for 8 cm x 8 cm LSC greenhouses at the optical density that resulted in the most lettuce production as well. (c) and (f) show the relative NPV at the optical density that resulted in the most energy production. Red, orange, and brown markers indicate results for LR305, CIS/ZnS, and Si greenhouses, respectively.

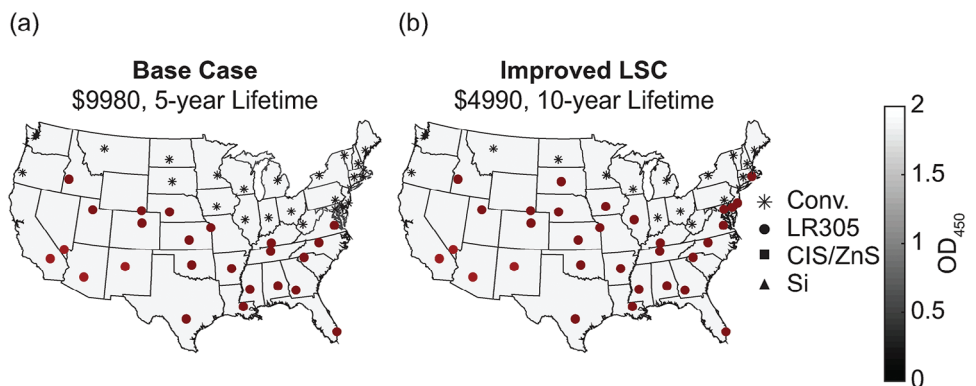


Figure 6. Greenhouses that were the most profitable in 48 locations across the continental United States at a) base case and b) improved LSC assumptions regarding LSC pricing and lifetime. If the optimum greenhouse was a conventional one, the data is plotted as a star. Otherwise, the data is plotted with a circle, a square, or a triangle for LR305, CIS/ZnS, or Si LSC greenhouses, respectively. The color of the marker corresponds to the luminophore's optical density, with brighter colors matching higher optical densities.

greenhouses were more profitable than conventional greenhouses in southern locations, the LR305 greenhouses were the optimized choice. The optical density that resulted in the optimum relative NPV was ≈ 1 for LR305, corresponding to the optical density that resulted in the ideal balance between high red fractions and sufficient transmitted light. LR305 greenhouses in the southwestern United States (Arizona, California, Nevada, and New Mexico) were most profitable with an optical density of 1.25 due to the higher insolation in these locations. These trends are reflected in Figure 4 as well, as LR305 greenhouses in climates with less sunlight (like MN) are optimized at an OD₄₅₀ closer to 1. Figure S13 (Supporting Information) shows the greenhouse that produced the most lettuce in each location; the optical densities that led to the highest annual fresh weight matched those that led to the highest NPV. Although LR305 greenhouses could produce more lettuce even in cold climates, the NPV of the LSC greenhouse at the base case assumptions could not surpass that of the conventional greenhouse due to the increase in heating demands.

We also probe the economic potential of LSC greenhouses under different scenarios. Developing low-cost manufacturing strategies for colloidal QDs as solar absorbers and other optoelectronic materials remains an active area of research for these materials.^[63] In contrast, molecular dyes, like LR305, have been commercially available for decades at lower costs.^[64] Furthermore, LR305 films have longer lifetimes, as they are stable in air for 10 years or more.^[65] Given future improvements to QD manufacturing, we assumed the cost of the LSC film was halved while the lifetime was doubled. The cost and lifetime were comparable to commercially available LR305 films embedded in poly (methyl methacrylate).^[19]

With these improvements, LSC greenhouses became the optimum choice in seven additional states, shown in Figure 6b. The LR305 greenhouses were still the most profitable, as the economic model was most sensitive to crop yield. Figure S13 (Supporting Information) shows that in most of the greenhouse sites, the LR305 greenhouses produced the most lettuce. In locations like Montana, the improvements to crop yield did not result in more profit. The high heating demands in these northernmost climates that are exacerbated by the addition of LSC films hinder the LSC greenhouses' profitability. Thus, the economic choice to implement LSC greenhouses is highly location-dependent but can be improved by lowering costs and increasing the lifetime of the LSC film.

3.5. Potential Directions for Future Model Development

As crop yield was the main determinant for NPV in this work, the growth model used mainly determined the economic potential of the LSC greenhouse. Utilizing growth models for other crops could result in differing conclusions for the economic viability of LSC greenhouses for those crops. This model also did not consider supplementary growing practices, such as supplemental LED lighting or deep winter greenhouses in cold climates like in MN. Advanced optical designs for near infrared radiation control could further improve heat management.^[66] The crop yield model was only used to calculate estimated fresh weights and did not consider the impacts of spectral shifting on the nutri-

tional value of the lettuce as well. This study did not consider the marketing and social implications of operating LSC greenhouses. Previous research has shown that consumers were more willing to pay for hydroponically grown lettuce upon receiving more information about this growing system's nutritional and sustainability benefits.^[67] By marketing the lettuce as a product produced in a solar-powered greenhouse, there may be the potential for additional crop revenue.

4. Conclusion

Increasing global populations require innovative methods to sustain them. Through agrivoltaic technologies, the needs for renewable energy and food production can be met in one plot of land. Greenhouses offer controlled environments for enhanced crop production but require much more energy than conventional farming. Agrivoltaic greenhouses can offset or completely meet this demand without significant detriment to crop yield. LSCs utilize commercial Si PV cells while providing the added benefits of enhancing power generation and shifting the transmitted spectrum of light.

In this paper, we provide design guidelines for LSC greenhouses through a comprehensive modeling framework, concurrently producing Bibb lettuce and renewable energy in the United States. Our model considers the greenhouse's environment (temperature and light), its energy demands, the power generated by two LSC designs with three luminophore candidates, crop growth, and economics. We found that crop yield was the most important determinant for the NPV in our economic model; LSC designs that maximized growth led to more profitable LSC greenhouses. LR305 greenhouses led to the highest transmitted red fractions, thus resulting in the most crop growth. CIS/ZnS has a higher quantum yield and reduced reabsorption losses; these greenhouses produced more energy, but additional profit from net metering was not as significant for the NPV calculation. Given LR305 greenhouses could produce the most lettuce, LSC greenhouses in a majority of the 48 locations studied were the most economically viable option. Upon improvements to the LSC cost and lifetime, the joint benefits of improved crop yield and energy offset supplied by the PV cells enabled economically realizable greenhouses in additional cold-climate locales. Our work supports future research and investment into agrivoltaic designs that integrate LSCs, as continuous improvements to LSC materials can bring these technologies closer to realization.

Supporting Information

Supporting Information is available from the Wiley Online Library or from the author.

Acknowledgements

The University of Minnesota – Twin Cities resides on Dakota land that was acquired through the Land Cession Treaties of 1837 and 1851. The authors acknowledge the legacies of violence, displacement, migration, and settlement that comes with our use of this land. Data were obtained from the National Aeronautics and Space Administration (NASA) Langley Research Center (LaRC) Prediction of Worldwide Energy Resource (POWER)

Project funded through the NASA Earth Science/Applied Science Program. The data were obtained from the POWER Project's Hourly 2.3.6 version on 2024/05/01. K.Q.L. was partially supported by the National Science Foundation Graduate Research Fellowship under grant no. 2237827 and received support from the University of Minnesota under the Ronald L. and Janet A. Christenson Chair in Renewable Energy.

Conflict of Interest

The authors declare no conflict of interest.

Author Contributions

All authors participated in the conception and design of the model and the simulations. K.Q.L. conducted all simulations and analyzed the data. K.H. contributed to the design of the shading algorithm. N.J.E. contributed to the crop growth model and greenhouse assumptions. K.Q.L., U.R.K., and V.E.F. drafted the manuscript. All authors read and edited the manuscript and gave approval to the final version.

Data Availability Statement

The data that support the findings of this study are openly available in DRUM at <https://doi.org/10.13020/r9zx-9m12>, reference number 1.

Keywords

agrivoltaics, greenhouses, luminescent solar concentrators, techno-economic analysis

Received: September 26, 2024
Revised: December 5, 2024
Published online:

- [1] "Agriculture and Food," <https://www.worldbank.org/en/topic/agriculture/overview>.
- [2] M. Walsh, P. Backlund, L. Buja, A. DeGaetano, R. Melnick, L. Prokopy, E. Tinkle, D. Todey, L. Ziska, *Climate Indicators for Agriculture*, United States Department of Agriculture, Climate Change Program Office, Washington D.C., 2020.
- [3] R. Hesampour, M. Taki, R. Fathi, M. Hassani, A. Halog, *Sci. Total Environ.* **2022**, 828, 154232.
- [4] F. Golzar, N. Heeren, S. Hellweg, R. Rosendal, *Sci. Total Environ.* **2019**, 675, 560.
- [5] C. F. Nicholson, K. Harbick, M. I. Gómez, N. S. Mattson, in *Food Supply Chains in Cities: Modern Tools for Circularity and Sustainability*, (Eds.: E. Aktas, M. Bourlakis), Springer International Publishing, Cham 2020, pp. 33.
- [6] J. Widmer, B. Christ, J. Grenz, L. Norgrove, *Renew. Sustainable Energy Rev.* **2024**, 192, 114277.
- [7] D. A. Chalkias, E. Stathatos, in *The Emergence of Agrivoltaics: Current Status, Challenges and Future Opportunities*, (Eds.: D. A. Chalkias, E. Stathatos), Springer International Publishing, Cham 2024, pp. 131.
- [8] A. V. Klokov, E. Y. Loktionov, Y. V. Loktionov, V. A. Panchenko, E. S. Sharaborova, *Energies* **2023**, 16, 3009.
- [9] G. A. Barron-Gafford, M. A. Pavao-Zuckerman, R. L. Minor, L. F. Sutter, I. Barnett-Moreno, D. T. Blackett, M. Thompson, K. Dimond, A. K. Gerlak, G. P. Nabhan, J. E. Macknick, *Nat. Sustain.* **2019**, 2, 848.
- [10] M. A. Woodhouse, B. Smith, A. Ramdas, R. M. Margolis, *Crystalline Silicon Photovoltaic Module Manufacturing Costs and Sustainable Pricing: 1H 2018 Benchmark and Cost Reduction Road Map*, National Renewable Energy Laboratory (NREL), Golden, CO, 2019.
- [11] S. Gorjian, E. Bousi, Ö. E. Özdemir, M. Trommsdorff, N. M. Kumar, A. Anand, K. Kant, S. S. Chopra, *Renew. Sustainable Energy Rev.* **2022**, 158, 112126.
- [12] A. Anttil, M. N. Beattie, C. Case, A. Chaudhary, B. D. Chrysler, M. G. Debije, S. Essig, D. K. Ferry, V. E. Ferry, M. Freitag, I. Gould, K. Hinzer, H. Hoppe, O. Inganäs, L. K. Jagadamma, M. H. Jee, R. K. Kostuk, D. Kirk, S. Kube, M. Lim, J. M. Luther, L. Mansfield, M. D. McGehee, D. N. Minh, P. Nain, M. O. Reese, A. Reinders, I. D. W. Samuel, W. van Sark, H. Savin, et al., *JPE* **2023**, 13, 042301.
- [13] E. F. Fernández, A. Villar-Fernández, J. Montes-Romero, L. Ruiz-Torres, P. M. Rodrigo, A. J. Manzaneda, F. Almonacid, *Appl. Energy* **2022**, 309, 118474.
- [14] M. Cossu, A. Yano, Z. Li, M. Onoe, H. Nakamura, T. Matsumoto, J. Nakata, *Appl. Energy* **2016**, 162, 1042.
- [15] A. Yano, M. Onoe, J. Nakata, *Biosyst. Eng.* **2014**, 122, 62.
- [16] M. Uchanski, T. Hickey, J. Bousselot, K. L. Barth, *Energies* **2023**, 16, 3012.
- [17] J. Keil, Y. Liu, U. Kortshagen, V. E. Ferry, *ACS Appl. Energy Mater.* **2021**, 4, 14102.
- [18] C. Corrado, S. W. Leow, M. Osborn, I. Carbone, K. Hellier, M. Short, G. Alers, S. A. Carter, *J. Renew. Sustainable Energy* **2016**, 8, 043502.
- [19] C. Corrado, S. W. Leow, M. Osborn, E. Chan, B. Balaban, S. A. Carter, *Sol. Energy Mater. Sol. Cells* **2013**, 111, 74.
- [20] L. Shen, R. Lou, Y. Park, Y. Guo, E. J. Stallknecht, Y. Xiao, D. Rieder, R. Yang, E. S. Runkle, X. Yin, *Nat. Food* **2021**, 2, 434.
- [21] D. Hebert, J. Boonekamp, C. H. Parrish, K. Ramasamy, N. S. Makarov, C. Castañeda, L. Schuddebeurs, H. McDaniel, M. R. Bergren, *Front. Chem.* **2022**, 10, 988227.
- [22] W. H. Weber, J. Lambe, *Appl. Opt.* **1976**, 15, 2299.
- [23] Y. Liu, J. Keil, V. E. Ferry, U. R. Kortshagen, *Adv. Sustainable Syst.* **2023**, 7, 2300107.
- [24] M. G. Debije, P. P. C. Verbunt, *Adv. Energy Mater.* **2012**, 2, 12.
- [25] M. G. Debije, V. A. Rajkumar, *Sol. Energy* **2015**, 122, 334.
- [26] L. D. Albright, A.-J. Both, A. J. Chiu, *Trans. ASAE* **2000**, 43, 421.
- [27] "National Aeronautics and Space Administration (NASA) Prediction of Worldwide Energy Resource (POWER) Project v2.0.0", <https://power.larc.nasa.gov/data-access-viewer/>, 2024.
- [28] D. J. Wojcicki, *Sol. Energy* **2015**, 112, 272.
- [29] C. H. Parrish, D. Hebert, A. Jackson, K. Ramasamy, H. McDaniel, G. A. Giacomelli, M. R. Bergren, *Commun. Biol.* **2021**, 4, 124.
- [30] D. C. J. Neo, M. M. X. Ong, Y. Y. Lee, E. J. Teo, Q. Ong, H. Tanoto, J. Xu, K. S. Ong, V. Suresh, *ACS Agric. Sci. Technol.* **2022**, 2, 3.
- [31] F. Pedron, M. Grifoni, M. Barbaferri, G. Petruzzelli, E. Franchi, C. Samà, L. Gila, S. Zanardi, S. Palmery, A. Proto, M. Voccante, *Appl. Sci.* **2021**, 11, 1923.
- [32] O. M. ten Kate, K. M. Hooning, E. van der Kolk, *Appl. Opt.* **2014**, 53, 5238.
- [33] D. Jurbergs, E. Rogojina, L. Mangolini, U. Kortshagen, *Appl. Phys. Lett.* **2006**, 88, 233116.
- [34] M. R. Bergren, N. S. Makarov, K. Ramasamy, A. Jackson, R. Guglielmetti, H. McDaniel, *ACS Energy Lett.* **2018**, 3, 520.
- [35] L. R. Wilson, B. S. Richards, *Appl. Opt.* **2009**, 48, 212.
- [36] B. Zhang, G. Lyu, E. A. Kelly, R. C. Evans, *Adv. Sci.* **2022**, 9, 2201160.
- [37] E. Fitz-Rodríguez, C. Kubota, G. A. Giacomelli, M. E. Tignor, S. B. Wilson, M. McMahon, *Comput. Electron. Agriculture* **2010**, 70, 105.
- [38] T. Soriano, J. I. Montero, M. C. Sánchez-Guerrero, E. Medrano, A. Antón, J. Hernández, M. I. Morales, N. Castilla, *Biosyst. Eng.* **2004**, 88, 243.
- [39] E. Ravishankar, R. E. Booth, J. A. Hollingsworth, H. Ade, H. Sederoff, J. F. DeCarolis, B. T. O'Connor, *Energy Environ. Sci.* **2022**, 15, 1659.

- [40] E. Ravishankar, R. E. Booth, C. Saravitz, H. Sederoff, H. W. Ade, B. T. O'Connor, *Joule* **2020**, 4, 490.
- [41] T. M. Robson, M. Pieristè, M. Durand, T. K. Kotilainen, P. J. Aphalo, *Plants, People, Planet* **2022**, 4, 314.
- [42] "Luminance Light Diffusing Greenhouse Plastic," <https://shrinkwrapcontainments.com/light-diffusing-greenhouse-plastic/>.
- [43] 2021 ASHRAE Handbook – Fundamentals, (Ed: H. E. Kennedy), American Society of Heating, Refrigerating and Air-Conditioning Engineers, **2021**.
- [44] M. S. Ahamed, H. Guo, K. Tanino, *Biosyst. Eng.* **2019**, 178, 9.
- [45] M. Eaton, T. Shelford, M. Cole, N. Mattson, *J. Cleaner Prod.* **2023**, 384, 135569.
- [46] C. F. Nicholson, M. Eaton, M. I. Gómez, N. S. Mattson, *Eur. Rev. Agricultural Economics* **2023**, 50, 1547.
- [47] M. Gargaro, R. J. Murphy, Z. M. Harris, *Plants* **2023**, 12, 2623.
- [48] N. Bumgarner, J. Buck, *JAH* **2016**, 18, 128.
- [49] E. J. Van Henten, *Agricultural Syst.* **1994**, 45, 55.
- [50] S. Zhen, M. van Iersel, B. Bugbee, *Front. Plant Sci.* **2021**, 12, 693445.
- [51] J. Liu, M. W. van Iersel, *Front. Plant Sci.* **2021**, 12, 619987.
- [52] D. Benetti, F. Rosei, *Nanoenergy Adv.* **2022**, 2, 222.
- [53] M. Abedi, X. Tan, E. J. Stallknecht, E. S. Runkle, J. F. Klausner, M. S. Murillo, A. Bénard, *Front. Plant Sci.* **2023**, 14, 1106576.
- [54] J. A. Hollingsworth, E. Ravishankar, B. O'Connor, J. X. Johnson, J. F. DeCarolis, *J. Indust. Ecol.* **2020**, 24, 234.
- [55] M. Kroggel, W. Lovichit, C. Kubota, C. Thomson, *Acta Hortic* **2012**, 952, 827.
- [56] J. Kneifel, D. Webb, in *Life Cycle Cost Manual for the Federal Energy Management Program*, National Institute Of Standards And Technology, Gaithersburg, MD **2020**.
- [57] "UbiGro Technical Data," <https://4764557.fs1.hubspotusercontent-na1.net/hubfs/4764557/UbiGro-Tech-Spec-Sheet-2022.pdf>.
- [58] "2023 Levelized Cost Of Energy+," <https://www.lazard.com/research-insights/2023-levelized-cost-of-energyplus/>.
- [59] H. E. Beck, N. E. Zimmermann, T. R. McVicar, N. Vergopolan, A. Berg, E. F. Wood, *Sci Data* **2018**, 5, 180214.
- [60] I. Sychugov, *Optica* **2019**, 6, 1046.
- [61] H.-Y. Chung, M.-Y. Chang, C.-C. Wu, W. Fang, *HortTechnology* **2018**, 28, 755.
- [62] M. Camporese, M. A. Najm, *Earth's Future* **2022**, 10, e2022EF002900.
- [63] A. R. Kirmani, J. M. Luther, M. Abolhasani, A. Amassian, *ACS Energy Lett.* **2020**, 5, 3069.
- [64] B. A. S. F. Group, 1993 *BASF Ann. Rep.* **1993**.
- [65] S. Carter, *Next Generation Print-Based Manufacturing for Photovoltaics and Solid State Lighting*, University of California, Santa Cruz, CA, **2012**.
- [66] G. H. Timmermans, S. Hemming, E. Baeza, E. A. J. van Thoor, A. P. H. J. Schenning, M. G. Debije, *Adv. Opt. Mater.* **2020**, 8, 2000738.
- [67] D. N. Gilmour, C. Bazzani, R. M. Nayga, H. A. Snell, *Agricultural Economics* **2019**, 50, 707.